narra j

Original Article

A network pharmacology approach to elucidate the anti-inflammatory and antioxidant effects of bitter leaf (*Vernonia amygdalina* Del.)

Illah Sailah[1], Trina E. Tallei[2*], Linda Safitri[1], Yulianida Tamala[1], Ernie Halimatushadyah[3], Dewi Ekatanti[4], Nur B. Maulydia[5] and Ismail Celik[6]

[1]Agroindustrial Engineering Study Program, Department of Agroindustrial Technology, Faculty of Agricultural Engineering and Technology, Institut Pertanian Bogor, Bogor, Indonesia; [2]Department of Biology, Faculty of Mathematics and Natural Sciences, Universitas Sam Ratulangi, Manado, Indonesia; [3]Pharmacy Study Program, Faculty of Health Sciences and Technology, Universitas Binawan, Jakarta, Indonesia; [4]Pharmacy Study Program, Faculty of Mathematics and Natural Sciences, Universitas Sam Ratulangi, Manado, Indonesia; [5]Graduate School of Mathematics and Applied Sciences, Universitas Syiah Kuala, Banda Aceh, Indonesia; [6]Department of Pharmaceutical Chemistry, Faculty of Pharmacy, Erciyes University, Kayseri, Turkey

*Corresponding author: trina_tallei@unsrat.ac.id

Abstract

The therapeutic potential of bitter leaf (*Vernonia amygdalina* Del.) has been established both empirically and in various scientific investigations. However, the molecular pathways related to its possible anti-inflammatory and antioxidant properties remain unclear. Therefore, the aim of this study was to elucidate the molecular interactions between bitter leaf's bioactive compounds and cellular targets involved in these activities. The compounds in bitter leaf were identified using gas chromatography-mass spectrometry (GC-MS) analysis, and subsequently, a network pharmacology approach was employed together with molecular docking and dynamics simulations. Acetonitrile (4.5%) and dimethylamine (4.972%) were the most prevalent compounds among the 38 identified by the GC-MS analysis of bitter leaf extract. The proto-oncogene tyrosine-protein kinase (SRC) demonstrated significant connectivity within the antioxidant network, highlighting its pivotal role in facilitating inter-protein communication. It also exhibited strategic positioning in anti-inflammatory mechanisms based on closeness centrality (0.385). The enrichment analysis suggested multifaceted mechanisms of bitter leaf compounds, including transcriptional regulation and diverse cellular targeting, indicating broad antioxidant and anti-inflammatory effects. Eicosapentaenoyl ethanolamide (EPEA) displayed strong interactions with multiple proteins, including SRC (-7.17 kcal/mol) and CYP3A4 (-6.88 kcal/mol). Moreover, EPEA demonstrated to form a stable interaction with SRC during a 100 ns simulation. In conclusion, the computational simulations revealed that the hypothetical antioxidant and anti-inflammatory actions of bitter leaf compounds were achieved by specifically targeting SRC. However, confirmation using either in vitro or in vivo techniques is necessary.

Keywords: Anti-inflammatory, antioxidant, bitter leaf, network pharmacology, *Vernonia amygdalina*

Introduction

Investigating the medical uses of natural compounds has attracted more and more interest in recent scientific research [1,2]. In this light, scientists are becoming interested in a native West African plant known as bitter leaf (*Vernonia amygdalina* Del.). Rich in phytochemicals and with

https://narraj.org/

Received: June 21, 2024 - Accepted: August 29, 2024 - Published online: October 7, 2024

a clearly bitter taste, this plant has long been employed in traditional medicine for many conditions [3-5]. Bitter leaf is thought to have notable molecules with anti-inflammatory and antioxidant properties. Such activities are essential pharmacological targets for various chronic diseases, including cardiovascular diseases, neurological disorders, and metabolic syndromes [6,7]. Therefore, investigating natural substances with anti-inflammatory and antioxidant characteristics presents great possibilities for creating creative treatment approaches to handle common health problems. According to earlier meta-analyses, substances such as curcumin and ursolic acid are effective substitutes for controlling oxidative stress and inflammation [8,9].

Although bitter leaf has a long history of traditional use and evidence supporting its efficacy, the precise molecular mechanisms behind its pharmacological effects remain unknown. Occasionally, conventional pharmacological methods are unable to completely comprehend the intricate interactions among bioactive compounds in plant extracts and their impact on cellular signaling pathways. Nevertheless, network pharmacology has emerged as a potent paradigm for comprehending the intricate interactions between drugs, targets, and diseases within biological networks through the application of computational methodologies and systems biology [10,11]. This approach systematically explores the molecular landscape underlying the therapeutic qualities of natural compounds through the use of computational techniques, network analysis, and the integration of omics data [12]. Furthermore, the predictive power of this method helps prioritize target proteins and candidate compounds for subsequent experimental validation, thereby accelerating the drug development process [13-15]. Previous studies have demonstrated that network pharmacology is an effective approach for identifying anti-inflammatory compounds derived from natural sources [14,16].

In order to investigate the molecular mechanisms and therapeutic potential of bitter leaf in natural medicine, a network pharmacology approach was implemented to characterize its antioxidant and anti-inflammatory properties. The aim of this study was to elucidate the complex network of interactions between the constituents of bitter leaf and their cellular targets by incorporating computational analyses. This method facilitates the rational application of its pharmacological properties in drug discovery and development and enhances comprehension of its properties. Additionally, molecular docking and molecular dynamics simulations were employed to clarify the binding interactions between bitter leaf components and their specific targets, thereby offering a more comprehensive understanding of their pharmacological effects.

Methods

Sample preparation

Fresh bitter leaves (1.5 kg) were trimmed into small fragments and air-dried in a greenhouse environment. The samples were collected from the Carang Pulang region in Dramaga, Bogor, Indonesia. The fragmented leaves were evenly spread on trays and left undisturbed for 20 hours until the moisture content reduced to less than 10%, as suggested previously [17]. The moisture content was assessed utilizing the Association of Official Analytical Chemists (AOAC) technique [18]. The greenhouse experienced fluctuations in temperature, averaging 32°C with 70% humidity.

Low-frequency ultrasonic waves (20–40 kHz) were used during ultrasonic-assisted extraction (UAE) to enhance the interaction between the solvent and the bitter leaf at room temperature [19]. The leaves were ground, measured, and combined with 80% methanol in a weight-to-volume ratio of 1:6 [20]. The sonication procedure was conducted at a power level of 200 W and 20 kHz frequency for 30 minutes. Afterward, the solvent was removed by subjecting it to a water bath at a 65°C for 30 minutes to 1 hour, resulting in a concentrated extract.

Gas chromatography-mass spectrometry (GC-MS) analysis

The volatile compounds were analyzed using gas chromatography-mass spectrometry (GC-MS), employing a Perkin Elmer Clarus 500 gas chromatograph coupled to a Perkin Elmer Clarus SQ 8S mass spectrometer. The separation was achieved using a Perkin Elmer Elite-5ms capillary column with dimensions of 30 meters length, 0.25 mm internal diameter, and 0.25 µm film thickness. Electron ionization was applied at 70 eV and the mass scanning range extended from

40 to 450 Da. Helium served as the carrier gas with the split mode set to 10:1. The injector temperature was maintained at 250°C, and a volume of 1 µL of sample was introduced, with a solvent delay of two minutes to facilitate the evaporation of the solvent prior to analysis. The oven settings for the analysis were as follows: the initial temperature was adjusted to 110°C and kept for two minutes. This was followed by a ramp rate of 10°C/min until reaching 200°C, which was then held for an additional two minutes. The temperature was increased gradually at a rate of 5°C per minute until it reached a final temperature of 280°C. Compounds were identified by comparing the mass spectra obtained with those in the NIST reference library. Additionally, where available, reference standards were used to confirm the identities of key compounds.

Network pharmacology

Target identification

The 24 substances were evaluated using SwissTargetPrediction to identify the most likely proteins or enzymes to be activated, with a cut-off probability value greater than 0 [21]. Using the GeneCards database with the keywords "inflammation" and "oxidation," all targets were gathered, and any duplicates with a relevance score greater than 5 were removed, resulting in a total of 500 candidates for each keyword to be used as biological targets [22]. All data were accessed in March 2024. A Venn diagram was employed to illustrate the overlap of active compounds with the targets from SwissTargetPrediction and GeneCards.

Analysis of protein-protein interactions (PPIs)

The identified overlapping targets were transferred to the STRING protein-protein interaction web database, selecting the human option (*Homo sapiens*) and highest confidence level (0.900) [23]. Network parameters of drug target PPIs, including degree and betweenness, were analyzed using Cytoscape 3.9.1 software (Institute for Systems Biology, Washington, USA) to understand the intermediary functions of the drug targets [24].

Functional enrichment of Gene Ontology (GO) and Kyoto Encyclopedia of Genes and Genomes (KEGG) pathway

The GO and KEGG pathway analyses were conducted using the Database for Annotation, Visualization and Integrated Discovery (DAVID) database [25]. The composition of GO comprises three ontologies: Biological Process (BP), Molecular Function (MF), and Cellular Component (CC) [26]. The importance of the enrichment outcome is determined using the -log10 transformation of the *p*-value. Afterwards, the collected results were visualized using the SRPlot tool using GO and KEGG enrichment plot [27].

Molecular docking

The ligand structures were obtained from PubChem in 3D format. For compounds available only in 2D format, their structures were converted to 3D using the MarvinSketch application. The protein structures, including protein SRC (PDB ID: 2H8H), protein CYP3A4 (PDB ID: 5TE8), protein ESR1 (PDB ID: 1X7R), and protein STAT3 (PDB ID: 6NJS), were validated based on Ramachandran plots using the Procheck program on the PDBsum web server. Each protein has a specific binding region, so the binding site or binding area was determined accordingly.

A grid box was used to define the size of the area on the protein where the compounds would be docked. The grid box was determined based on the native ligand binding area of the protein. The grid box size was obtained using the Biovia Discovery Studio application. Molecular docking was performed using Gnina through Google Colab (https://github.com/gnina/gnina) [28]. The molecular docking process began by uploading each protein and ligand file into the Gnina folder, followed by executing the process using predefined text commands, which were modified as needed.

Molecular dynamics simulations

The molecular dynamics simulations (MDS) were performed following previously established procedures [29]. Gromacs 2020.4 [30] was used to explore the dynamic behavior [31] and binding interactions of the ligand-protein complex. The necessary input files for MDS were

generated via the CHARMM-GUI [32] server. The topology of the ligand-protein complex was constructed utilizing CHARMM36m force fields [33] and the TIP3 water model [34]. A rectangular box with 3D periodic boundary conditions was selected for solvation, maintaining a 15 Å distance between the box edges and the protein-protein complex [31]. The system was neutralized with 0.15 M KCl using the Monte Carlo method. Energy minimization was executed with the steepest descent integrator over 5000 steps. System equilibration was carried out with 0.5 ns NVT/NPT ensembles at 303.15 K and 1 atm pressure, employing the Nose–Hoover thermostat [35] and Parrinello–Rahman barostat [36], respectively. The leap-frog integration method facilitated 100 ns molecular dynamics (MD) simulations, comprising 1000 frames with 2 fs time steps [37,38]. The superimposition of the complex configuration at 0ns, 50ns, and 100ns was performed using PyMOL [39].

Results

Profile of bitter leaf extract metabolite compounds

GC-MS analysis identified 38 compounds in the extract of bitter leaf (**Table 1**). Compounds such as dimethylamine and acetonitrile appeared multiple times at different retention times and scan numbers, indicating their high prevalence in the sample. The most abundant compounds are dimethylamine and acetonitrile with retention areas of 4.972% and 4.517%, respectively. The identified compounds were classified into 13 groups based on their main functional groups in the molecule. Firstly, the amine group consists of dimethylamine, which appeared twice. Next, the amide group was represented by butanamide, 3-(2-. Nitrile is present in 4,4-ethylenedioxy-pentanenitrile and acetonitrile, appearing four times. The aldehyde group consists of 2-formylhistamine and 3,7-dimethylnona-2,6-dienal. The alcohol group was represented by 2-heptanol, 6-amino-2-, 1-octanol, 2,7-dimethyl-, and 1-octen-3-ol. The alcohol group includes 2-heptanol, 6-amino-2-, 1-octanol, 2,7-dimethyl-, and 1-octen-3-ol. Ester compounds include 10-undecenoic acid, octyl ester, and valeric acid, 2-tridecyl ester. Ketones were represented by 10-undecen-4-one, 2,2,6,6-tetramethyl-, while other compounds include oxirane, octyl-, and 3-propionyloxytridecane. Hydrocarbons are present in decane, 2,4,6-trimethyl-, tridecane, 5-methyl-, octadecane, 1-(ethenyloxy)-, 6-methyloctadecane, and 1,4-dimethyl-3-n-octadecylcyclohexane. Carboxylic acids consist of octanoic acid, 7-oxo-, oxalic acid, butyl ester, and dodecanoic acid, 3-hydroxy-. Diazena amide was presented in the form of diazenecarboximidoyl. Finally, other compounds include hydrazinecarboxamide, cyclopentane, 1-acetyl-, 2-butyltetrahydrofuran, 3-methyl-1-dodecyn-3-ol, and trans-4-pentylcyclohexanecarboxylic acid (**Table 1**).

Table 1. The compound profile derived from the bitter leaf extract based on gas chromatography-mass spectrometry (GC-MS) analysis

Retention time (min)	Scan	Area %	Compound name
2.043	9	3.012	2-Formylhistamine
2.864	173	3.345	Dimethylamine
4.304	461	1.627	Dimethylamine
4.955	591	1.024	4,4-Ethylenedioxy-pentanenitrile
5.89	778	0.613	2-Heptanol, 6-amino-2-
6.605	921	0.614	Hydrazinecarboxamide
33.231	6244	0.581	3,7-Decadiene, 2,9-
33.366	6271	1.342	Decane, 2,4,6-trimethyl-
33.451	6288	2.048	1-Octanol, 2,7-dimethyl-
33.511	6300	1.05	Tridecane, 5-methyl-
33.541	6306	0.939	Acetonitrile
33.621	6322	1.226	Acetonitrile
33.656	6329	0.78	Eicosapentaenoyl ethanolamide
34.177	6433	0.629	Diazenecarboximidoyl
34.227	6443	0.775	Octanoic acid, 7-oxo-
34.292	6456	1.58	Octadecane, 1-(ethenyloxy)-
34.332	6464	0.673	Butanamide, 3-(2-
34.392	6476	0.672	Cyclopentane, 1-acetyl-
34.532	6504	0.896	Acetonitrile
34.677	6533	0.657	1-Octen-3-ol

Retention time (min)	Scan	Area %	Compound name
34.722	6542	0.754	10-Undecenoic acid, octyl ester
34.872	6572	1.075	10-Undecen-4-one, 2,2,6,6-tetramethyl-
34.922	6582	0.614	Oxirane, octyl-
34.987	6595	1.228	3-Propionyloxytridecane
35.037	6605	1.426	1,2-15,16-Diepoxyhexadecane
35.092	6616	0.728	Acetonitrile
35.137	6625	0.952	3,7-Dimethylnona-2,6-dienal
35.187	6635	1.139	2-(3-Cyclohexylaminopropylamino) ethylthiophosphate
35.262	6650	1.1	Butanoic acid, 2-hexenyl ester, (E)-
35.327	6663	0.711	Cyclooctanone, oxime
35.467	6691	0.699	trans-4-Pentylcyclohexanecarboxylic acid
35.492	6696	0.656	Oxalic acid, butyl
35.517	6701	1.19	6-Methyloctadecane
35.572	6712	0.607	1,4-Dimethyl-3-n-octadecylcyclohexane
35.647	6727	0.825	3-Methyl-1-dodecyn-3-ol
35.752	6748	1.116	2-Butyltetrahydrofuran
35.832	6764	1.266	Valeric acid, 2-tridecyl ester
35.857	6769	0.606	1,2-Cyclopentanediol, 3-methyl
35.937	6785	0.58	Dodecanoic acid, 3-hydroxy-
35.972	6792	0.728	Acetonitrile

Potential active compounds and targets

SwissTargetPrediction analysis identified a total of 404 protein targets associated with the compounds present in the bitter leaf extract, indicating the potential bioactivity of these compounds against various protein targets. GeneCards was subsequently employed to select proteins linked to inflammatory and oxidative activities within cells, with a strict cut-off (>5 relevance score) applied to ensure the selection of highly relevant proteins. This process led to the identification of 500 proteins for each activity.

Analysis using Venn diagrams (**Figure 1**) revealed the overlaps between the protein targets of the bitter leaf extract and those associated with inflammation and oxidative stress. Specifically, 63 proteins overlapped with inflammation-related proteins and 62 proteins overlapped with oxidative stress-related proteins. This indicated the potential involvement of the bitter leaf extract in modulating these biological pathways. Additionally, 24 protein targets were found to be common among all three components: the bitter leaf extract, inflammation, and oxidative stress. This finding suggested the potential multi-target effects of the extract in mitigating both inflammatory and oxidative responses within cells.

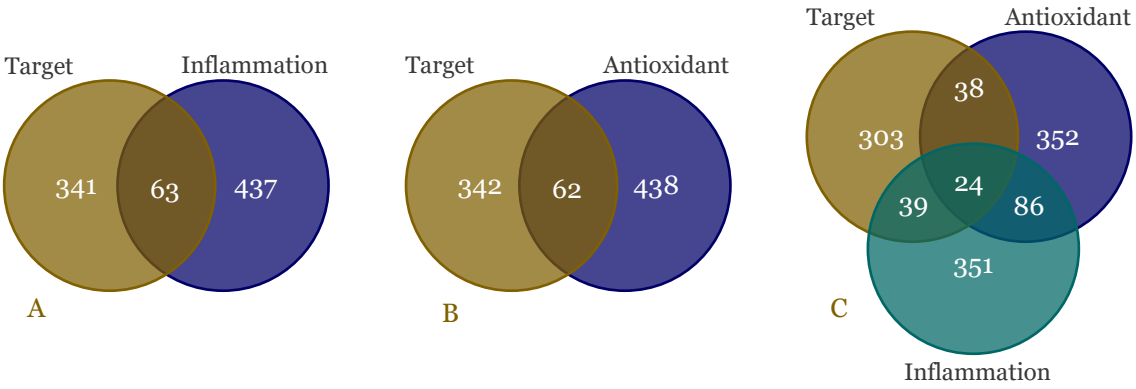

Figure 1. Venn diagram analysis illustrates the overlap between bitter leaf extract protein targets and those linked to inflammation and oxidative stress. Sixty-three proteins exhibited overlap with inflammation (A), while 62 proteins overlapped with oxidative stress (B), implying the potential modulation of pathways. Furthermore, 24 targets were shared among bitter leaf extract, inflammation, and oxidative stress, indicating the possibility of multi-target effects in alleviating both cellular responses (C).

Protein-protein interactions (PPIs)

PPIs in antioxidant activity

The top 15 protein-protein interactions (PPIs) linked to antioxidant activity are presented in **Table 2**. The results of the PPI network highlighted distinctive features for the SRC and STAT3 proteins within the antioxidant network. SRC exhibited a high degree of 15, indicating its interactions with 15 other proteins in the network. While SRC served as a bridge connecting other proteins to some extent, as indicated by its betweenness centrality score of 0.117 (closeness centrality: 0.385). STAT3 had a degree of 10, which was slightly lower than SRC.

Table 2. The top 15 protein-protein interactions (PPI) linked to antioxidant activity

Protein name	Degree	Betweenness centrality	Closeness centrality
SRC	15	0.117	0.385
CYP3A4	12	0.216	0.392
ESR1	12	0.266	0.427
STAT3	10	0.279	0.431
CYP2C19	9	0.135	0.382
CYP2C9	9	0.105	0.373
HSP90AA1	9	0.047	0.364
MAOB	9	0.083	0.329
MAOA	9	0.083	0.329
AKT1	9	0.023	0.367
CTNNB1	8	0.023	0.338
EGFR	8	0.016	0.359
MAPK8	8	0.054	0.364
PIK3CA	8	0.018	0.341
BCL2	7	0.050	0.341

However, its betweenness centrality score (0.789) was higher than SRC, where the closeness centrality value was 0.431. The illustration of the connectivity network of proteins related to antioxidant activity is presented in **Figure 2**.

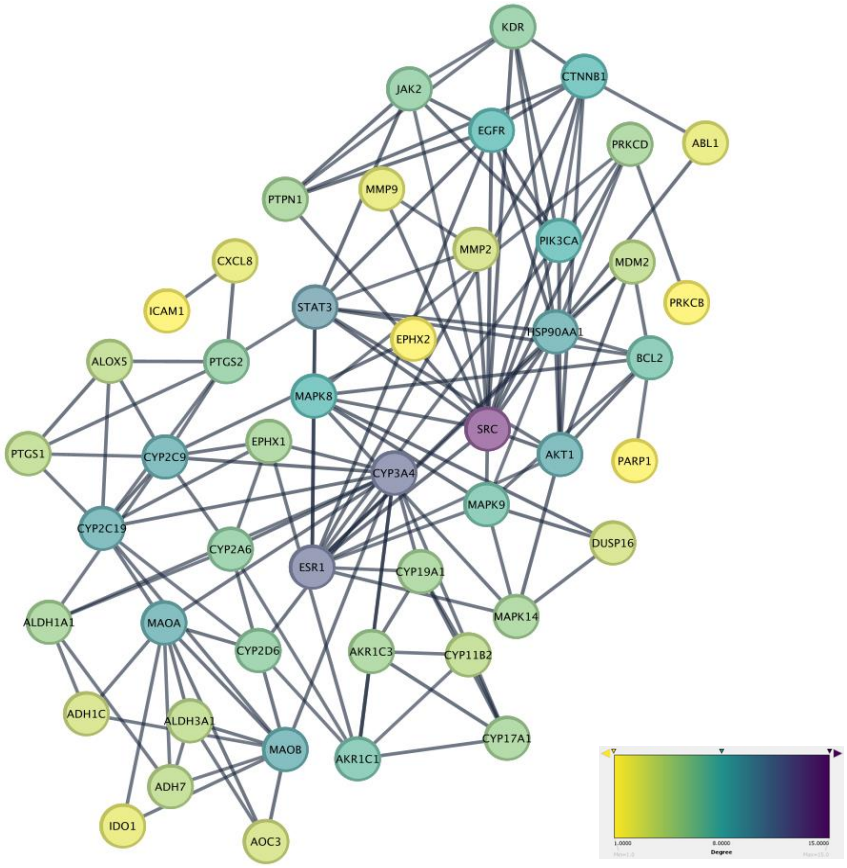

Figure 2. The PPI network associated with antioxidant activity. The increasing purple color indicated higher degrees, while the increasingly yellow color signified lower degrees.

PPIs in anti-inflammatory activity

The top 15 protein-protein interactions (PPIs) associated with anti-inflammatory activity are presented in **Table 3**. STAT3 emerged as a central player with extensive interactions, reflected in its high degree value of 14. SRC exhibited strong interconnectedness within the network, with a degree of 13. PIK3CA and ESR1 both had a degree of 9, reflecting their similar roles in anti-inflammatory mechanisms. Regarding betweenness centrality, STAT3 and CXCL8 stood out with the highest values, suggesting their crucial intermediary roles in connecting proteins, while SRC and MMP9 also exhibited higher betweenness centrality.

Table 3. The top 15 protein-protein interactions linked to anti-inflammatory activity

Protein name	Degree	Betweenness centrality	Closeness centrality
STAT3	14	0.582	0.377
SRC	13	0.218	0.336
PIK3CA	9	0.019	0.278
ESR1	9	0.029	0.315
AKT1	8	0.032	0.310
EGFR	7	0.012	0.308
MAPK8	7	0.069	0.310
CTNNB1	6	0.001	0.270
JAK2	6	0.010	0.303
MMP9	6	0.141	0.269
CXCL8	5	0.473	0.308
JAK1	5	0.005	0.290
CREBBP	5	0.010	0.303
PRKCD	4	0.010	0.267
MMP2	4	0.093	0.308

In terms of closeness centrality, STAT3, ESR1, and MAPK8 displayed high values, indicating their strategic positions within the network and potential influence over other proteins. The illustration of the key proteins involved in anti-inflammatory activity and their connectivity within the network are presented in **Figure 3**.

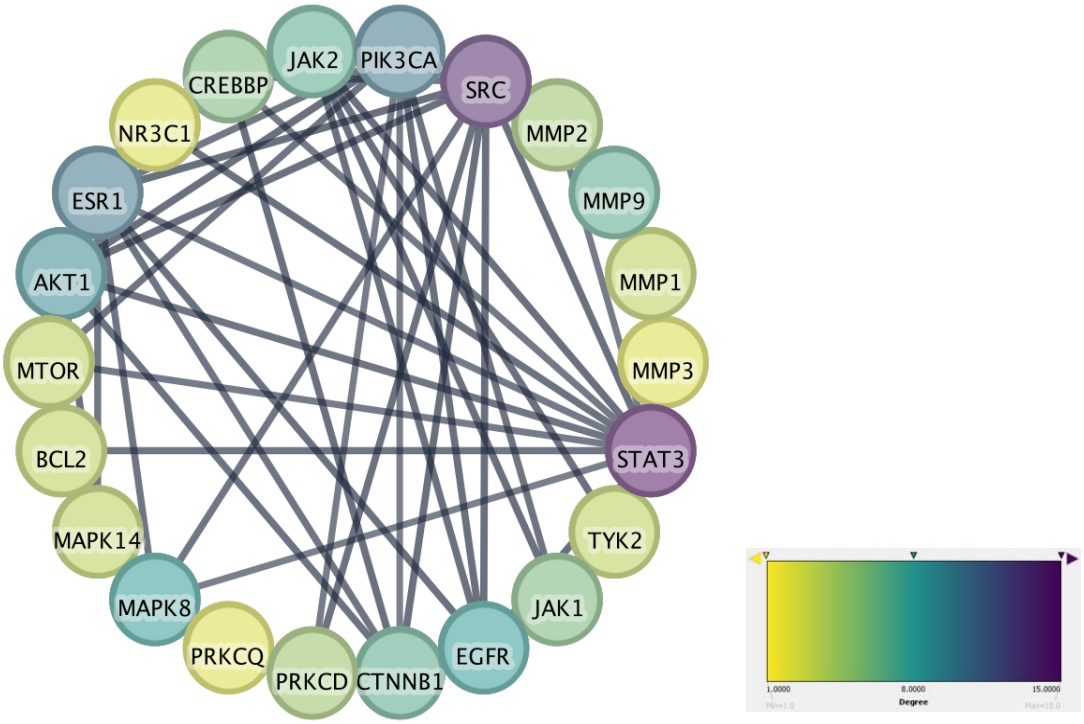

Figure 3. The PPI network associated with anti-inflammatory activity. The increasing purple color indicates higher degrees, while the increasingly yellow color signifies lower degrees.

Enrichment of GO and KEGG pathway

Enrichment of GO and KEGG pathway linked to antioxidant activity

Understanding gene functions and their interrelationships across three domains—cellular component (CC), molecular function (MF), and biological process (BP)—is made possible by gene ontology (GO). Ten important GO terms were found for every compound in the GO enrichment analysis of 342 possible antioxidant targets (p<0.01, **Figure 4A**). Bitter leaf compounds appeared to exert their antioxidant effects through several molecular regulatory mechanisms, including the positive regulation of transcription, the negative regulation of gene expression, and the inhibition of apoptosis.

These compounds target a range of cellular components such as the cytoplasm, plasma membrane, cytosol, membrane, and mitochondrion, suggesting extensive antioxidant activity. Targeting a spectrum of cellular components, including the cytoplasm, plasma membrane, cytosol, membrane, and mitochondrion, these molecules imply great antioxidant action. Enzyme binding, protein phosphatase binding, oxidoreductase activity, and protein serine/threonine kinase activity are among the molecular roles connected with these molecules.

These properties suggest that several pathways, including cellular signaling, metabolism, and redox control, govern the antioxidant actions of bitter leaf. Additionally, the KEGG pathway enrichment analysis highlighted that pathways related to chemical carcinogenesis and receptor activation were significantly enriched among the top ten entries, where the results are presented in **Figure 4B**. This finding suggested that the antioxidant properties of bitter leaf are connected to pathways involved in chemical-induced cancer development and receptor activation, pointing to potential mechanisms through which bitter leaf exerts its beneficial effects.

Enrichment of GO and KEGG pathway linked to anti-inflammatory activity

For each compound, the GO enrichment analysis of 341 potential anti-inflammatory targets identified 10 significant GO terms (p<0.01, **Figure 5A**). The findings suggested that bitter leaf compounds may help reduce inflammation through various biological mechanisms. These include suppressing gene expression, regulating signal transduction, and promoting the transcription of DNA. By targeting key parts of the cell, such as the plasma membrane, cytoplasm, cytosol, nucleus, and nucleoplasm, these compounds can influence inflammatory responses at multiple levels. The molecular functions linked to bitter leaf compounds, like protein kinase activity, ATP binding, and enzyme binding, point to several pathways that may help to reduce inflammation. These activities highlighted their potential role in important signaling processes and enzymatic reactions related to inflammation.

The KEGG pathway enrichment analysis further supported these findings by highlighting significant enrichment of pathways associated with cancer, hepatitis B, and Kaposi's sarcoma-associated herpesvirus (KSHV) infection (**Figure 5B**). This enrichment suggested that the anti-inflammatory effects of bitter leaf compounds may intersect with pathways involved in cancer progression and viral infections. The presence of these pathways suggested potential interactions or shared molecular mechanisms between inflammatory responses, cancer, and viral infections, emphasizing the complex nature of the anti-inflammatory effects of bitter leaf.

Molecular docking

The analysis of ligand-protein interactions revealed several important insights, as illustrated in the heatmap (**Figure 6**). Quinazoline demonstrated a strong connection with the SRC protein, with a binding-free energy (BFE) of -9.76 kcal/mol, indicating a high level of affinity. Similarly, Midazolam demonstrated a strong affinity to the CYP3A4 protein, with a BFE of -11.93 kcal/mol. Genistein also had a very strong interaction with the ESR1 protein, showing a BFE of -9.43 kcal/mol. Additionally, SD36 had a strong interaction with the STAT3 protein, with a BFE of -9.12 kcal/mol. Quinazoline naturally binds to SRC, Midazolam to CYP3A4, Genistein to ESR1, and SD36 to STAT3. Bitter leaf extract compounds, such as eicosapentaenoyl ethanolamide (EPEA), also displayed strong interactions with proteins like SRC (-7.17 kcal/mol) and CYP3A4 (-6.88 kcal/mol) but showed weaker affinity with ESR1 (-3.41 kcal/mol) and STAT3 (-4.56 kcal/mol). Additionally, trans-4-Pentylcyclohexanecarboxylic acid interacted with ESR1, yielding a BFE of -7.02 kcal/mol.

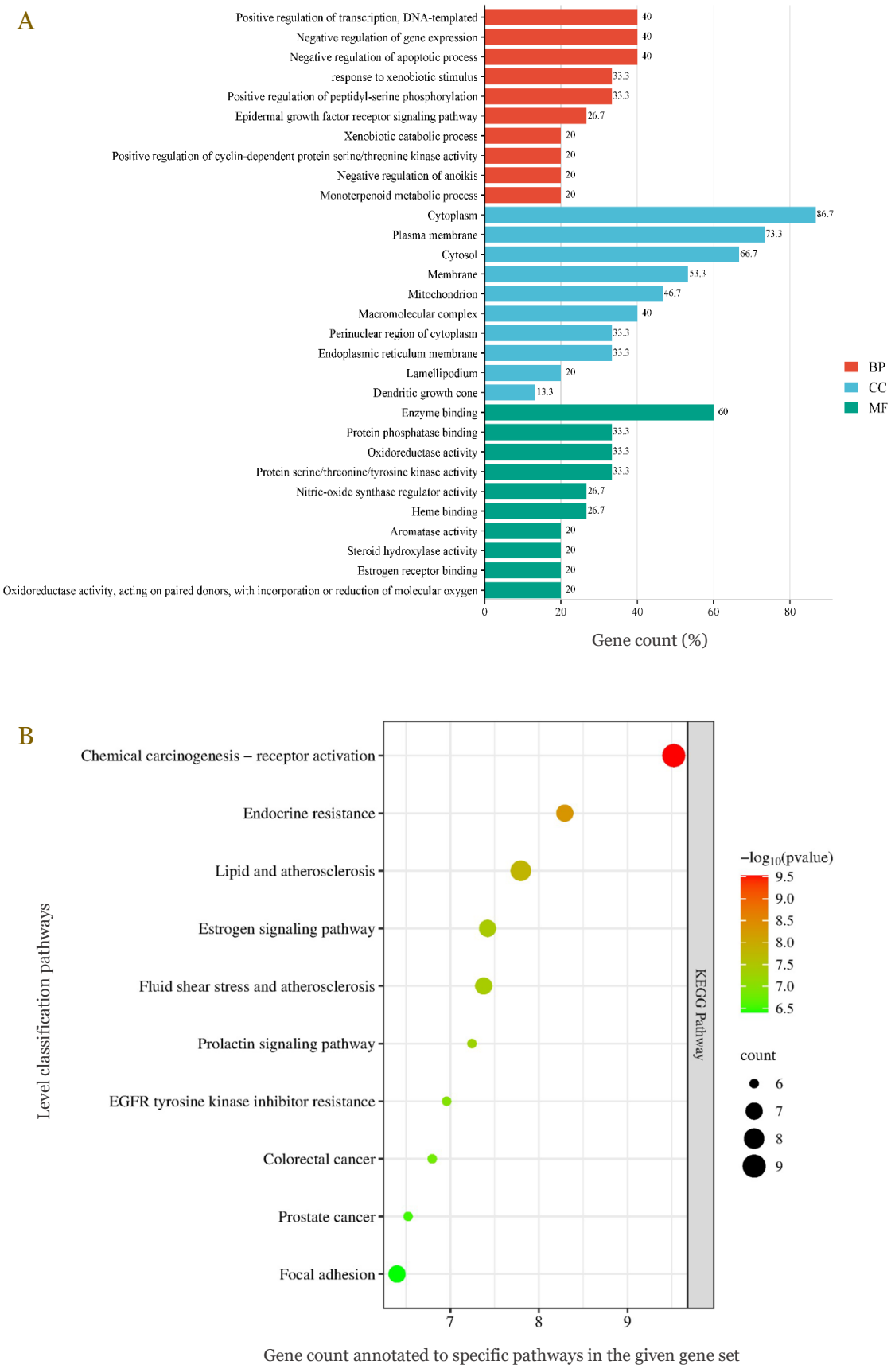

Figure 4. GO and KEGG pathway enrichment related to antioxidant activity. (A) Gene Ontology (GO) analysis; (B) Kyoto Encyclopedia of Genes and Genomes (KEGG) pathway.

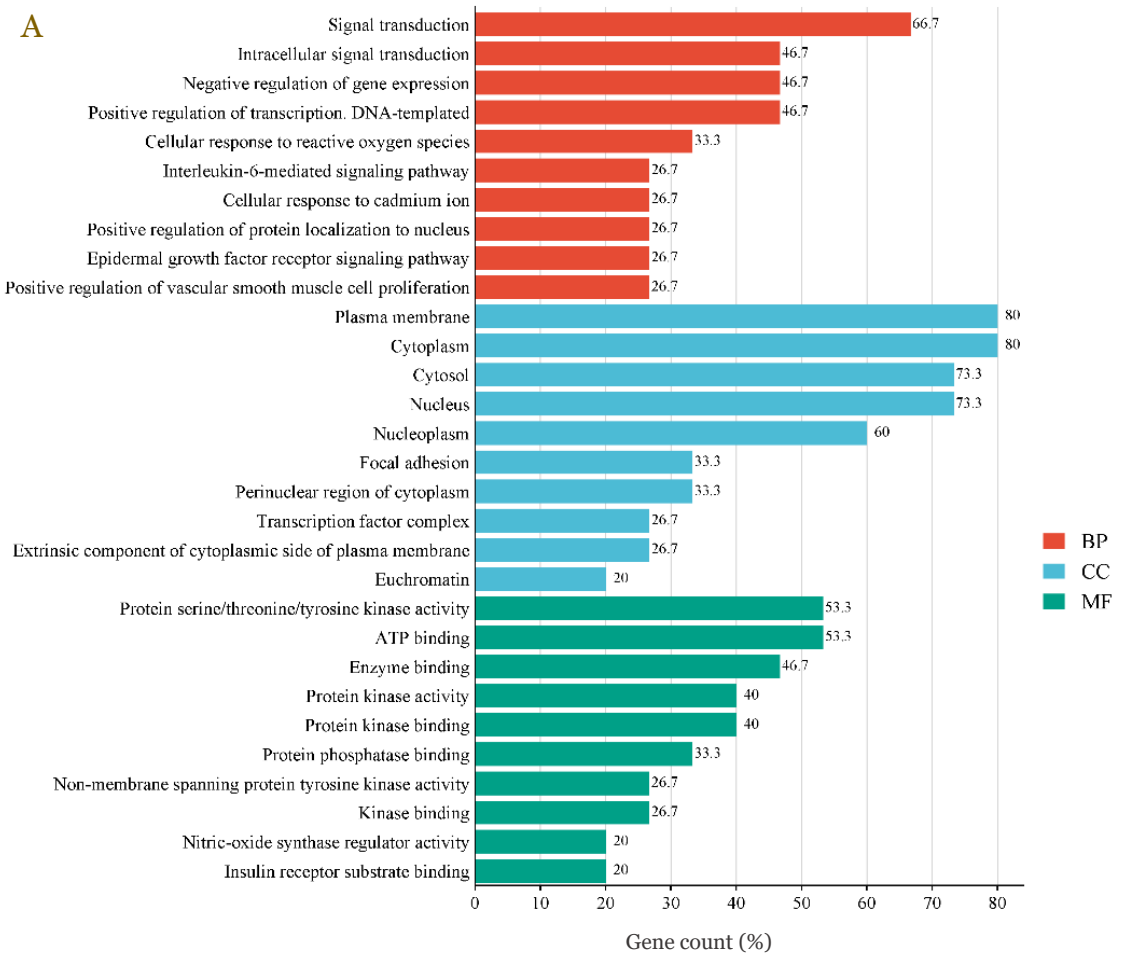

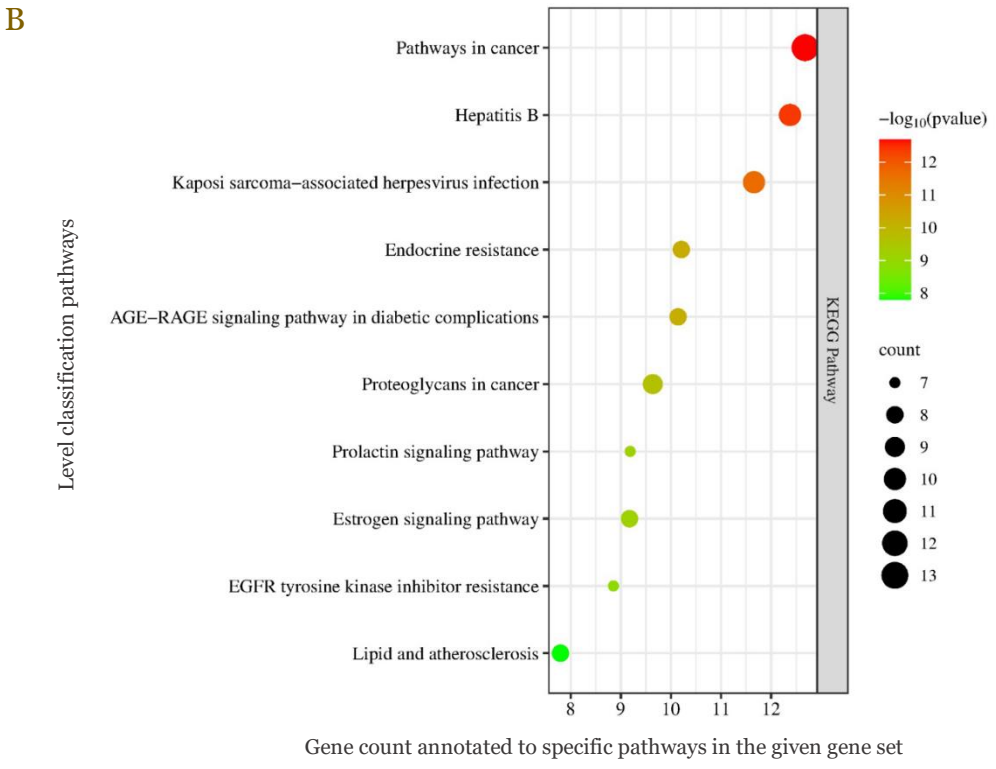

Figure 5. GO and KEGG Pathway Enrichment related to anti-inflammatory activity. (A) Gene Ontology (GO) analysis; (B) Kyoto Encyclopedia of Genes and Genomes (KEGG) pathways.

Figure 6. Heatmap of the interactions between compounds present in bitter leaf and target proteins (SRC, CYP3A4, ESR1, and STAT3). The values indicate the binding-free energy (BFE) in kcal/mol. The lower the BFE value, the stronger the interaction between the compound and the target protein.

Both Quinazoline-SRC and EPEA-SRC complexes are involved in a combination of Van der Waals forces, hydrogen bonds, and Pi interactions (**Figure 7**). Importantly, EPEA-SRC showed a wider variety of interactions, which might lead to more flexible and resilient binding, with binding-free energies (BFEs) of -9.76 kcal/mol and -7.17 kcal/mol, respectively. In a similar way, Midazolam-CYP3A4 and EPEA-CYP3A4 formed extensive Van der Waals and hydrogen bonds. The additional salt bridges and charge interactions in Midazolam-CYP3A4 suggested a stronger and more targeted binding, with BFEs of -11.93 kcal/mol. When looking at Genistein-ESR1 and trans-4-Pentylcyclohexanecarboxylic acid-ESR1, significant interactions are observed, where Pi interactions in Genistein-ESR1 likely contribute to a more stable binding, reflected by BFEs of -9.43 kcal/mol. The SD36-STAT3 and EPEA-STAT3 complexes showed different interaction patterns, with SD36-STAT3 exhibiting stronger binding, while EPEA-STAT3 had weaker binding, with BFEs of -9.12 kcal/mol and -4.59 kcal/mol, respectively (**Figure 7**).

Molecular dynamics simulation

The EPEA-SRC complex was chosen for an evaluation of their interaction stability through molecular dynamics simulations (MDS) due to its possibility of having strong and adaptable binding. Throughout the simulation, RMSD values fluctuated within the range of approximately 0.1 nm to 0.3 nm (**Figure 8A**). Notably, the protein backbone achieved a relatively stable conformation after initial fluctuations, with minor deviations suggesting dynamic stability (**Figure 8A**). The root-mean-square fluctuation (RMSF) of values varies considerably among different residues, with peaks indicating regions of higher flexibility within the protein structure (**Figure 8B**). Terminal residues exhibited particularly high fluctuations, a common occurrence reflecting inherent flexibility (**Figure 8B**).

The RMSD of the ligand EPEA exhibited higher variation, ranging from approximately 0.1 nm to 0.35 nm (**Figure 8C**). The graph suggested periods of both stability and significant movement relative to the protein, hinting at dynamic interactions and potential conformational changes during binding (**Figure 8C**). The number of hydrogen bonds formed between the ligand and the protein fluctuates between 0 and 4 (**Figure 8D**). Spikes indicated instances of multiple

A

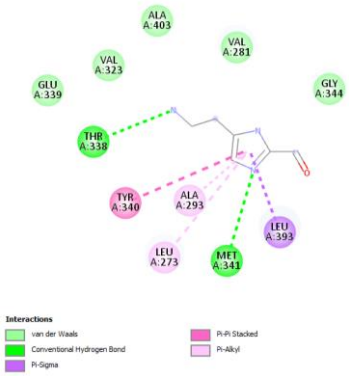

-9.76 kcal/mol

B

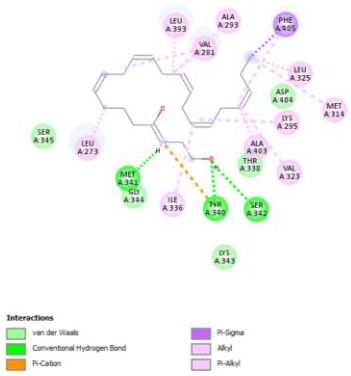

-7.17 kcal/mol

C

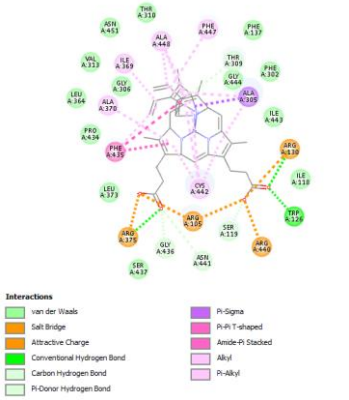

-11.93 kcal/mol

D

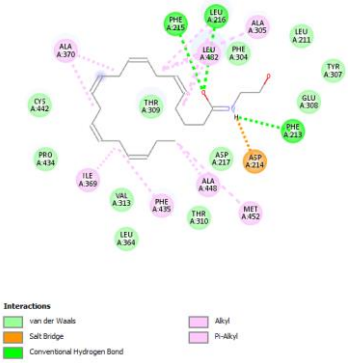

-6.88 kcal/mol

E

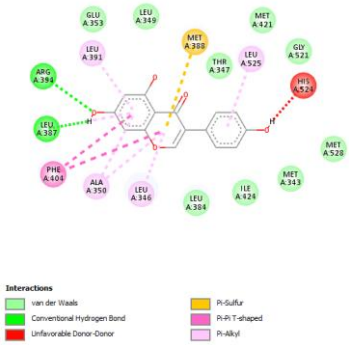

-9.43 kcal/mol

F

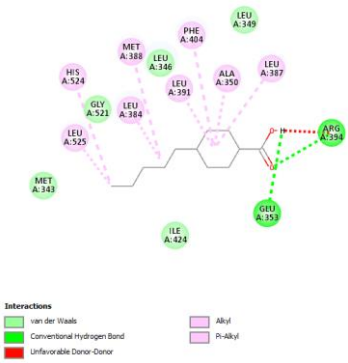

-7.02 kcal/mol

G

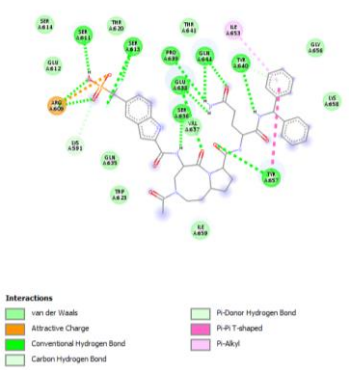

-9.12 kcal/mol

H

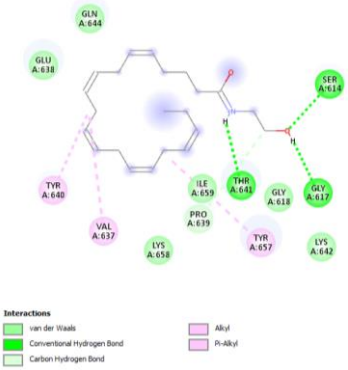

-4.59 kcal/mol

Figure 7. Molecular interactions between various ligands and their target receptors: (A) quinazoline with SRC; (B) EPEA with SRC; (C) midazolam with CYP3A4; (D) EPEA with CYP3A4; (E) genistein with ESR1; (F) trans-4-Pentylcyclohexanecarboxylic acid with ESR1; (G) SD36 with STAT3; (H) EPEA with STAT3.

hydrogen bonds, potentially corresponding to tighter binding periods. This variability suggested multiple dissociation and reassociation events between the ligand and the protein binding site (**Figure 8D**).

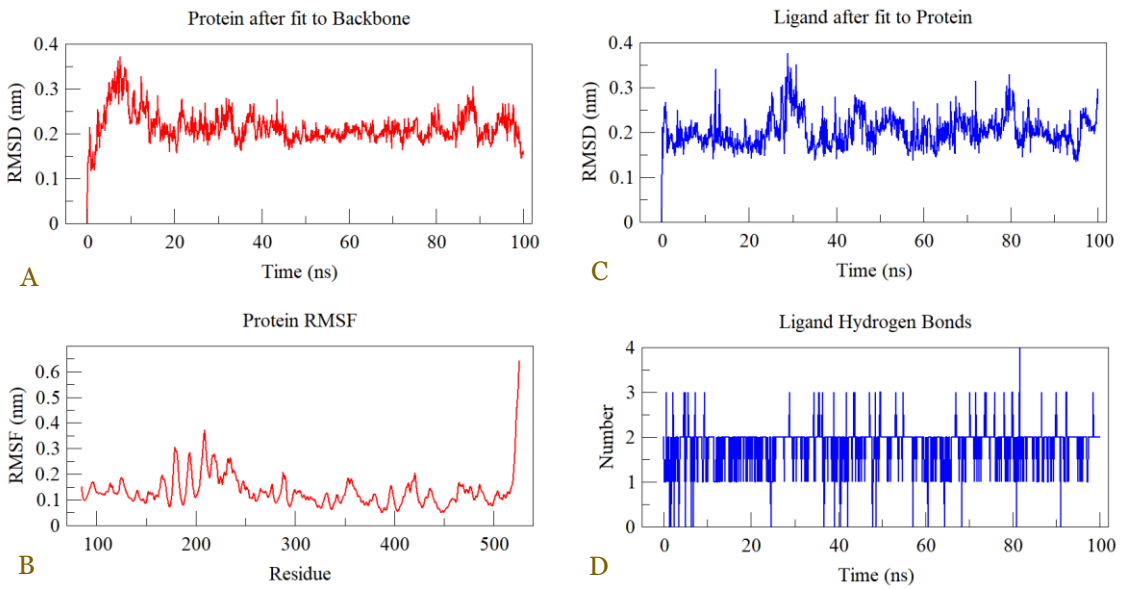

Figure 8. A molecular dynamic simulation trajectory of the ligand EPEA and the receptor SRC kinase from 0 ns to 100 ns. (A) Protein after fit to the backbone; (B) protein RMSF; (C) ligand after fitting to protein; and (D) ligand hydrogen bonds.

The investigation into the positioning of the ligand EPEA and its interactions with the SRC kinase receptor has yielded significant findings across these time points (**Figure 9**). Initially, at 0 ns, EPEA was found ensconced within the binding pocket of the SRC kinase receptor, establishing key interactions through van der Waals forces, including higher conventional hydrogen bonding (H-bonds) with specific amino acids such as Tyr A:340 and Met A:341. By the 50 ns mark, while the ligand persisted within the binding pocket, there were discernible shifts, possibly indicating dynamic rearrangements.

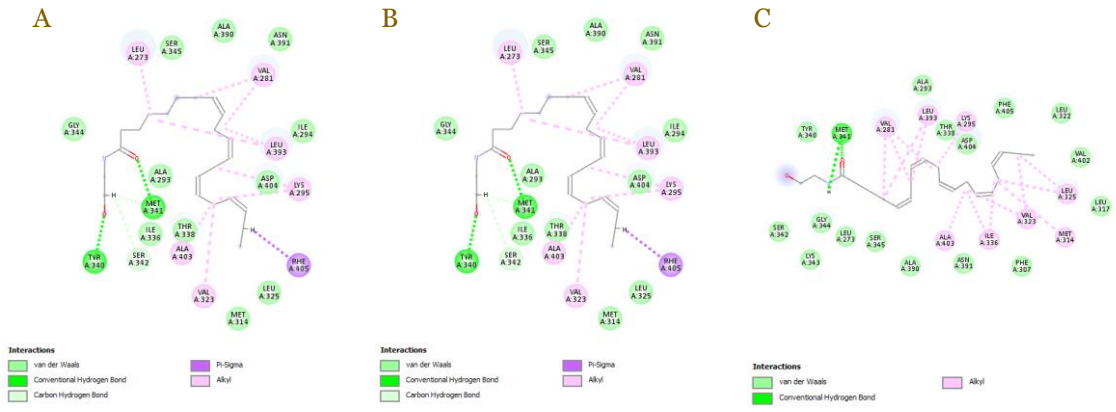

Figure 9. The position of the ligand EPEA within the binding pocket of the SRC kinase receptor over the course of the simulation. (A) At 0 ns; (B) at 50 ns; and (C) at 100 ns. The interactions, particularly the hydrogen bonds and van der Waals interactions, play a crucial role in stabilizing the ligand. The persistence of these interactions suggests a stable binding affinity, which is essential for the ligand's efficacy.

Despite these changes, interactions, particularly van der Waals forces, continued to be significant, with persistent hydrogen bonding, especially with Met A:341 and Tyr A:340. Additionally, new interactions may have emerged, or existing ones may have strengthened. As the simulation reached 100 ns, the ligand stayed centrally located within the binding pocket, showing

extensive interactions with surrounding amino acids through van der Waals forces. A significant hydrogen bond persisted with Met A:341, along with interactions such as a carbon hydrogen bond with Tyr A:340 (**Figure 9**).

The superimposition between the complex at 0 ns, 50 ns, and 100 ns is presented in **Figure 10**. The ligand's position appears stable, indicating a relatively unchanged complex configuration, with an RMSD value remaining within the range of 1.680 Å. This indicated that the interaction between the ligand and the receptor remains consistent throughout the observed simulation period.

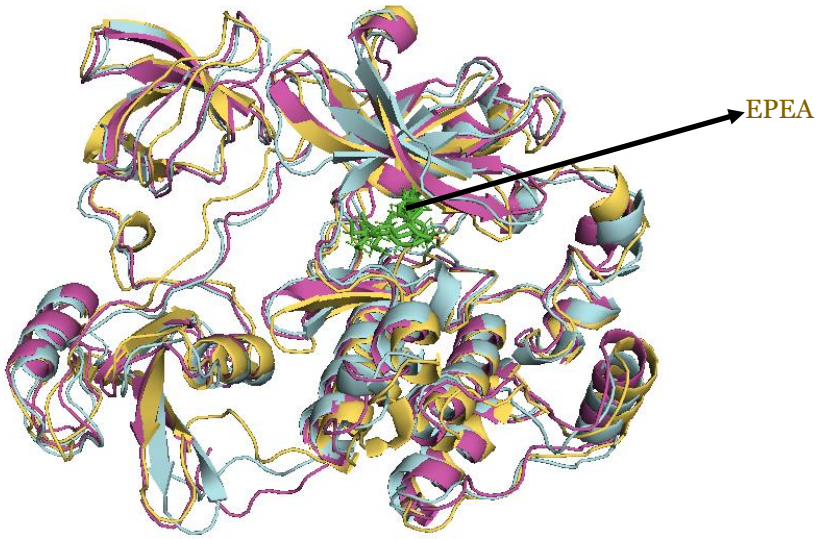

Figure 10. Superimposition of the complex EPEA-SRC at 0 ns (magenta), 50 ns (yellow), and 100 ns (cyan) reveal stable ligand positioning with minimal variation, maintaining an RMSD of 1.680 Å, indicating consistent ligand-receptor interaction throughout the simulation.

Discussion

This study investigated *Vernonia amygdalina*, commonly known as bitter leaf, to evaluate its potential as an antioxidant and anti-inflammatory agent. The evaluation employed computational modeling techniques, including network pharmacology, molecular docking, and molecular dynamics simulations. According to GC-MS analysis, the extract from greenhouse-dried leaves revealed the presence of 38 distinct compounds, categorized into 13 compound groups. Among these compounds, dimethylamine and acetonitrile were the most abundant. Notably, dimethylamine has previously been reported in this plant [40,41]. According to the Swisstarget prediction tool, herein, bitter leaf extract may have significant therapeutic potential in combating inflammation and oxidative stress by modulating multiple cellular pathways simultaneously. As suggested previously, this tool predicts the most likely protein targets of a small molecule based on similarities with known drugs [21,42].

The present study identified SRC and STAT3 as key elements in the antioxidant network, with SRC exhibiting strong connectivity and STAT3 acting as a crucial link. These findings emphasized their roles in antioxidant activities. Previous research has revealed that SRC, a non-receptor tyrosine kinase, plays a crucial role in several cellular processes, such as cell growth, movement, attachment, and survival [43-45]. SRC plays a role in managing oxidative stress and inflammation by controlling antioxidant defense systems and the production of reactive oxygen species (ROS) [46,47]. When activated by pro-inflammatory cytokines, SRC can contribute to cancer progression. However, inhibiting SRC has been shown to lower inflammation and oxidative stress in situations like salt-induced hypertension [48,49]. Meanwhile, STAT3, a transcription factor, is key in how cells respond to cytokines and growth factors [50]. It regulates

gene expression related to oxidative stress and inflammation, with its activation leading to an increase in antioxidant enzymes and anti-inflammatory substances [51,52].

The previous study has demonstrated that quinolines and quinazolines effectively inhibit SRC kinase activity [53]. For instance, quinazoline inhibits SRC kinase, a key player in the MAPK signaling pathway, by preventing it from functioning. This inhibition stops SRC kinase from activating downstream signaling molecules, which in turn reduces cytokine production. Considering EPEA's strong binding affinity for SRC kinase, it is plausible that EPEA could similarly interfere with the MAPK signaling pathway, leading to a reduction in cytokine production, which suggests its potential as a therapeutic agent.

Herein, SRC and STAT3 were identified as key targets in the antioxidant network, which may be modulated by the bioactive compounds in bitter leaf. This modulation could strengthen cellular defenses, reduce oxidative damage, and alleviate inflammation, thereby enhancing the leaf's overall antioxidant capacity. Understanding the interactions between bitter leaf compounds and SRC/STAT3 pathways could provide insights into its molecular mechanisms and aid in developing antioxidant-rich supplements or pharmaceutical interventions for oxidative stress-related diseases. A previous study suggested that modulating SRC and STAT3 activity can impact cell growth, inflammation, cancer progression, angiogenesis, and immune responses, making them attractive targets for therapeutic interventions [54].

The present study demonstrated that EPEA exhibited a high binding affinity for both SRC protein and CYP3A4, with binding free energies of -7.17 and -6.88 kcal/mol, respectively. This finding indicated significant pharmacological implications. When EPEA binds to SRC with a strong affinity, it could potentially influence these signaling pathways. For instance, it could affect the SRC kinase-mediated signaling pathways involved in tumor progression, invasion, and metastasis in various cancers, including breast cancer [55]. Moreover, SRC interacts with other proteins to promote their degradation or protect them from degradation, which could also be influenced by EPEA binding.

CYP3A4 is a member of the cytochrome P450 superfamily of enzymes, which are involved in the metabolism of various substances, including drugs and endogenous compounds [56]. The present study suggested that EPEA binding to CYP3A4 may influence the enzyme's metabolic activity. For instance, CYP3A4 also possesses epoxygenase activity, metabolizing arachidonic acid to epoxyeicosatrienoic acids (EETs), which have a wide range of activities, including the promotion of certain types of cancers [57,58]. EPEA binding could potentially influence this process. Furthermore, EPEA could be converted to other metabolites via CYP epoxygenases, which could have various biological effects. The exact consequences of EPEA binding to SRC and CYP3A4 depend on the cellular context and require further research.

However, while binding scores indicate the strength of interaction, they do not necessarily predict the biological outcome, which can be influenced by various factors. Consequently, the stability of the EPEA-SRC interaction was additionally examined through MDS, a computational technique that visualizes the dynamics of atoms and molecules within biological systems [59]. The results indicated that during the 100 ns simulation, EPEA remained bound to the same site on the protein, signifying its strong affinity for SRC. This was corroborated by the presence of multiple types of bonds, particularly hydrogen bonding and covalent bonds, reinforcing this interaction [60].

The suggested actions by which EPEA suppresses the activity of several proteins engaged in inflammation are presented in **Figure 11**. The compounds inhibit SRC kinase, resulting in lower SRC substrate phosphorylation. This inhibition prevents the activation of the nuclear factor kappa B (NF-κB), mitogen-activated protein kinase (MAPK), and signal transducer and activator of transcription (STAT) pathways, reducing the expression of genes that induce inflammation. Furthermore, EPEA reduces the activity of STAT and ESR1 (ERα) proteins. STAT3 is a transcription factor that, upon activation by Janus kinase (JAK) associated with membrane receptors, facilitates the promotion of inflammatory responses [61]. ESR1 can also modulate the immune response by reducing estrogen signaling that causes excessive inflammation. Additionally, ESR1 can promote controlled inflammation, and its inhibition might weaken this response [62]. As a result, the production of pro-inflammatory cytokines is then reduced, resulting in fewer inflammatory cells migrating and adhering to the site of inflammation. The

inflammatory reaction eventually subsides, and the tissue returns to its normal state. This process is known as the resolution of inflammation.

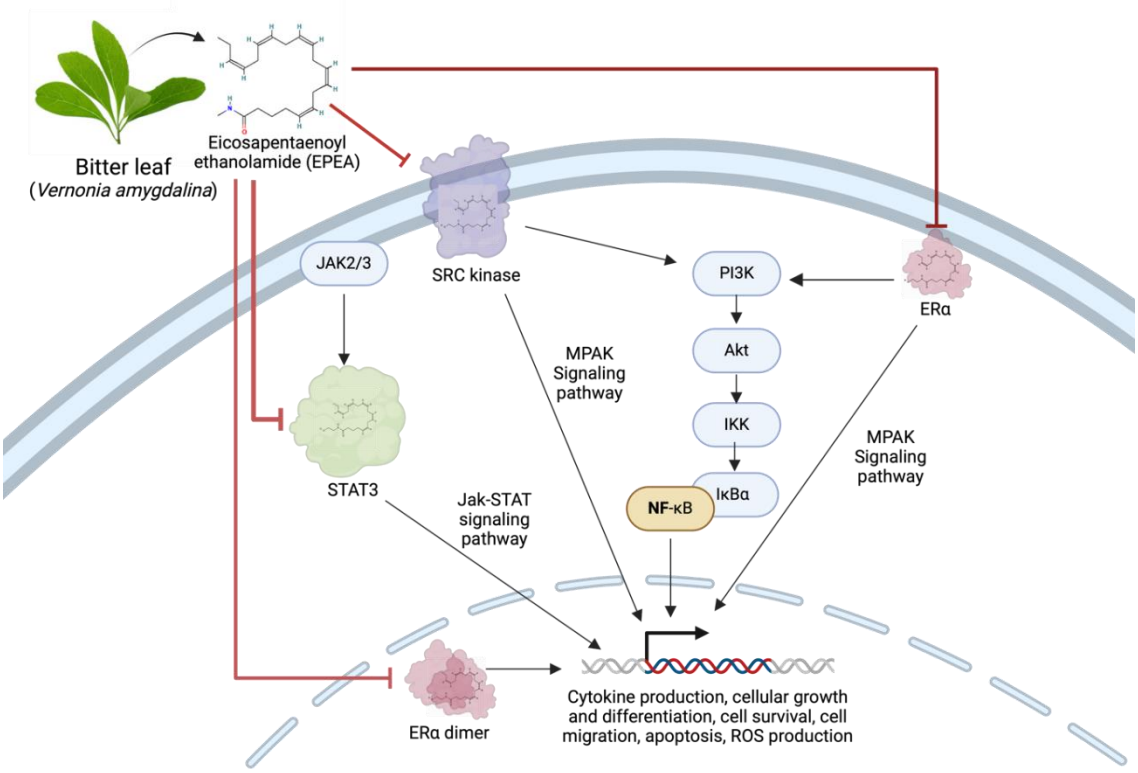

Figure 11. EPEA acts as an anti-inflammatory agent by inhibiting SRC kinase, STAT3, and ESR1 (ERα) activities, thereby preventing expression of inflammation-inducing genes. These activities decrease pro-inflammatory cytokines and reduce cell migration and adhesion at inflammation sites.

The antioxidant activities of EPEA are associated with its capacity to decrease oxidative stress, a crucial element in the onset and advancement of inflammation. When the body cannot neutralize reactive oxygen species (ROS) using antioxidants, a condition known as oxidative stress results. Acting as an antioxidant, EPEA neutralizes ROS, therefore reducing oxidative stress and the ensuing inflammation. This wide activity of EPEA emphasizes its anti-inflammatory properties.

Though these findings implied a strong and lasting interaction between EPEA and SRC, it is essential to recognize that the biological consequences of this interaction can be influenced by various factors and are not solely determined by binding scores or interaction stability. Many other factors can influence the outcome. To truly grasp the significance of this interaction, more research is needed—this includes experimental validation, studying how it affects SRC activity and related signaling pathways, and evaluating its potential for therapeutic use.

It also should be noted that the present study's reliance on computational simulation may not fully reflect in vivo conditions, potentially affecting the accuracy of observed interactions and effects. GC-MS analysis also has limitations, including challenges with complex samples and non-volatile compounds that can hinder accurate identification and quantification. Variations in sample preparation and instrument calibration can further impact accuracy. Additionally, the research did not address the bioavailability and metabolic pathways of EPEA and other bitter leaf compounds, which are crucial for assessing their efficacy and safety in clinical use. The scope was limited to specific targets like SRC and CYP3A4, leaving out other potential mechanisms and targets. Experimental validation is needed to confirm their biological relevance. Moreover, the complexity of natural compounds presents challenges in isolating their specific effects, and the interactions among various bioactive components in bitter leaf were not fully explored.

Conclusion

The findings of the present study suggest that SRC is a key therapeutical target of bitter leaf's bioactive compounds, particularly EPEA. Its strong binding to SRC supports its potential as a promising anti-inflammatory agent by inhibiting SRC kinase, which in turn affects STAT3 and ESR1, thereby reducing inflammatory pathways and pro-inflammatory cytokines. Additionally, EPEA's antioxidant properties mitigate oxidative stress. However, the findings from the present study warrant further investigation on bitter leaf's pharmacological mechanisms, bioavailability, and formulation strategies.

Ethics approval

Not required.

Competing interests

All the authors declare that there are no conflicts of interest.

Funding

This study was funded by Institut Pertanian Bogor under the National Collaboration Research Scheme (Ri-Na) Lecturer Research Assignment for the fiscal year 2023–2024, with grant number 498/IT3.D10/PT.01.03/P/B/2023.

Underlying data

The authors confirm that the data supporting the conclusions of this research are included in the manuscript. Furthermore, additional derived data can be requested from the corresponding author.

Acknowledgement

The numerical calculations presented in this article were partially conducted using resources from TÜBİTAK (The Scientific and Technological Research Council of Turkey) at ULAKBİM (Turkish Academic Network and Information Centre) and the High Performance and Grid Computing Centre (TRUBA resources).

How to cite

Sailah I, Tallei TE, Safitri L, *et al*. A network pharmacology approach to elucidate the anti-inflammatory and antioxidant effects of bitter leaf (*Vernonia amygdalina* Del.). Narra J 2024; 4 (3): e1016 - http://doi.org/10.52225/narra.v4i3.1016.

References

1. Chaachouay N, Zidane L. Plant-derived natural products: A source for drug discovery and development. Drugs Drug Candidates 2024;3(1):184-207.
2. Abas AH, Tallei TE, Idroes R, *et al.* Ficus minahassae (Teijsm & de Vriese) Miq.: A fig full of health benefits from North Sulawesi, Indonesia: A mini review. Malacca Pharm 2023;1(1):1-7.
3. Edo GI, Samuel PO, Jikah AN, *et al.* Biological and bioactive components of bitter leaf (*Vernonia amygdalina* leaf): Insight on health and nutritional benefits. A review. Food Chem Adv 2023;3:100488.
4. Degu S, Meresa A, Animaw Z, *et al.* Vernonia amygdalina: A comprehensive review of the nutritional makeup, traditional medicinal use, and pharmacology of isolated phytochemicals and compounds. Front Nat Prod 2024;3:1347855.
5. Alara OR, Abdurahman NH, Ukaegbu CI, *et al.* Extraction and characterization of bioactive compounds in *Vernonia amygdalina* leaf ethanolic extract comparing Soxhlet and microwave-assisted extraction techniques. J Taibah Univ Sci 2019;13(1):414-422.
6. Biswas SK. Does the interdependence between oxidative stress and inflammation explain the antioxidant paradox? Oxid Med Cell Longev 2016;2016:5698931.
7. Nediani C, Dinu M. Oxidative stress and inflammation as targets for novel preventive and therapeutic approaches in non-communicable diseases II. Antioxidants 2022;11(5):824.

8. Zhao M, Wu F, Tang Z, *et al.* Anti-inflammatory and antioxidant activity of ursolic acid: A systematic review and meta-analysis. Front Pharmacol 2023;14:1256946.
9. Dehzad MJ, Ghalandari H, Nouri M, *et al.* Antioxidant and anti-inflammatory effects of curcumin/turmeric supplementation in adults: A GRADE-assessed systematic review and dose–response meta-analysis of randomized controlled trials. Cytokine 2023;164:156144.
10. Chandran U, Mehendale N, Patil S, *et al.* Network pharmacology. Innov Approaches Drug Discov 2017:127-164.
11. Noor F, ul Qamar M, Ashfaq UA, *et al.* Network pharmacology approach for medicinal plants: Review and assessment. Pharmaceuticals 2022;15(5):572.
12. Yang M, Chen JL, Xu LW, *et al.* Navigating traditional Chinese medicine network pharmacology and computational tools. Evid Based Complement Alternat Med 2013;2013:731969.
13. Li L, Yang L, Yang L, *et al.* Network pharmacology: A bright guiding light on the way to explore the personalized precise medication of traditional Chinese medicine. Chin Med 2023;18(1):146.
14. Tallei TE, Fatimawali, Adam AA, *et al.* Molecular insights into the anti-inflammatory activity of fermented pineapple juice using multimodal computational studies. Arch Pharm (Weinheim) 2024;357(1):e2300422.
15. Pendong CHA, Suoth EJ, Fatimawali F, *et al.* Network pharmacology approach to understanding the antidiabetic effects of pineapple peel hexane extract. Malacca Pharm 2024;2(1):24-32.
16. Khairan K, Maulydia NB, Faddillah V, *et al.* Uncovering anti-inflammatory potential of *Lantana camara* Linn: Network pharmacology and in vitro studies. Narra J 2024;4(2):e894.
17. Raja KS, Taip FS, Azmi MMZ, *et al.* Effect of pre-treatment and different drying methods on the physicochemical properties of *Carica papaya* L. leaf powder. J Saudi Soc Agric Sci 2019;18(2):150-156.
18. Latimer GW Jr. Official methods of analysis of AOAC international (22nd edition). Online; AOAC Publications; 2023.
19. Kumar K, Srivastav S, Sharanagat VS. Ultrasound assisted extraction (UAE) of bioactive compounds from fruit and vegetable processing by-products: A review. Ultrason Sonochem 2021;70:105325.
20. Adiwibowo MT, Herayati H, Erlangga K, *et al.* Pengaruh metode dan waktu ekstraksi terhadap kualitas dan kuantitas saponin dalam ekstrak buah, daun, dan tangkai daun Belimbing Wuluh (*Avverhoa bilimbi* L.) untuk aplikasi detergen. J Integrasi Proses 2020;9(2):44-50.
21. Daina A, Michielin O, Zoete V. SwissTargetPrediction: Updated data and new features for efficient prediction of protein targets of small molecules. Nucleic Acids Res 2019;47(W1):W357-W364.
22. Stelzer G, Rosen N, Plaschkes I, *et al.* The GeneCards suite: From gene data mining to disease genome sequence analyses. Curr Protoc Bioinforma 2016;2016(6):1.30.1-1.30.33.
23. Szklarczyk D, Kirsch R, Koutrouli M, *et al.* The STRING database in 2023: Protein-protein association networks and functional enrichment analyses for any sequenced genome of interest. Nucleic Acids Res 2023;51(1D):D638-D646.
24. Shannon P, Markiel A, Ozier O, *et al.* Cytoscape: A software environment for integrated models. Genome Res 2003;13(22):426.
25. Sherman BT, Hao M, Qiu J, *et al.* DAVID: A web server for functional enrichment analysis and functional annotation of gene lists (2021 update). Nucleic Acids Res 2022;50(W1):W216-W221.
26. Ashburner M, Ball CA, Blake JA, *et al.* Gene ontology: Tool for the unification of biology. The gene ontology consortium. Nat Genet 2000;25(1):25-29.
27. Tang D, Chen M, Huang X, *et al.* SRplot: A free online platform for data visualization and graphing. PLoS One 2023;18(11):e0294236.
28. McNutt AT, Francoeur P, Aggarwal R, *et al.* GNINA 1.0: Molecular docking with deep learning. J Cheminformatics 2021;13(1):43.
29. Celik I, Tallei TE. A computational comparative analysis of the binding mechanism of molnupiravir's active metabolite to RNA-dependent RNA polymerase of wild-type and Delta subvariant AY.4 of SARS-CoV-2. J Cell Biochem 2022;123(4):807-818.
30. Abraham MJ, Murtola T, Schulz R, *et al.* GROMACS: High performance molecular simulations through multi-level parallelism from laptops to supercomputers. SoftwareX 2015;1-2:19-25.
31. Ghaheh HS, Ganjalikhany MR, Yaghmaei P, *et al.* Improving the solubility, activity, and stability of reteplase using in silico design of new variants. Res Pharm Sci 2019;14(4):359-368.
32. Jo S, Kim T, Iyer VG, *et al.* CHARMM-GUI: A web-based graphical user interface for CHARMM. J Comput Chem 2008;29(11):1859-1865.
33. Huang J, Rauscher S, Nawrocki G, *et al.* CHARMM36m: An improved force field for folded and intrinsically disordered proteins. Nat Methods 2017;14(1):71-73.

34. Mark P, Nilsson L. Structure and dynamics of the TIP3P, SPC, and SPC/E water models at 298 K. J Phys Chem A 2001;105(43):9954-9960.
35. Evans DJ, Holian BL. The Nose–Hoover thermostat. J Chem Phys 1985;83(8):4069-4074.
36. Parrinello M, Rahman A. Polymorphic transitions in single crystals: A new molecular dynamics method. J Appl Phys 1981;52(12):7182-7190.
37. Celik I, Khan A, Dwivany FM, *et al.* Computational prediction of the effect of mutations in the receptor-binding domain on the interaction between SARS-CoV-2 and human ACE2. Mol Divers 2022;26(6):3309-3324.
38. Hessel SS, Dwivany FM, Zainuddin IM, *et al.* A computational simulation appraisal of banana lectin as a potential anti-SARS-CoV-2 candidate by targeting the receptor-binding domain. J Genet Eng Biotechnol 2023;21(1):148.
39. Schrödinger L, DeLano W. PyMOL 2020. Available from: http://www.pymol.org/pymol. Accessed: 15 January 2024.
40. Imaga NA, Iheagwam FN, Asibe C, *et al.* Antidiabetic modulatory effects of Vernonia amygdalina and *Allium sativum* combined extract in streptozotocin-induced diabetic rats. Vegetos 2023;36(2):615-625.
41. Ugbogu EA, Emmanuel O, Dike ED, *et al.* The phytochemistry, ethnobotanical, and pharmacological potentials of the medicinal *Plant-Vernonia amygdalina* L. (bitter Leaf). Clin Complement Med Pharmacol 2021;1(1):100006.
42. Gfeller D, Grosdidier A, Wirth M, *et al.* SwissTargetPrediction: A web server for target prediction of bioactive small molecules. Nucleic Acids Res 2014;42(Web Server issue):W32-W38.
43. Roskoski R. Src protein-tyrosine kinase structure, mechanism, and small molecule inhibitors. Pharmacol Res 2015;94:9-25.
44. Ortiz MA, Mikhailova T, Li X, *et al.* Src family kinases, adaptor proteins and the actin cytoskeleton in epithelial-to-mesenchymal transition. Cell Commun Signal 2021;19(1):67.
45. De Kock L, Freson K. The (Patho)biology of SRC kinase in platelets and megakaryocytes. Medicina 2020;56(12):633.
46. Hussain M, Ikram W, Ikram U. Role of c-Src and reactive oxygen species in cardiovascular diseases. Mol Genet Genomics 2023;298(2):315-328.
47. Jin W. Regulation of Src family kinases during colorectal cancer development and its clinical implications. Cancers 2020;12(5):1339.
48. Liu ST, Pham H, Pandol SJ, *et al.* Src as the link between inflammation and cancer. Front Physiol 2013;4:416.
49. Yang Q, Yu XJ, Su Q, *et al.* Blockade of c-Src within the paraventricular nucleus attenuates inflammatory cytokines and oxidative stress in the mechanism of the TLR4 signal pathway in salt-induced hypertension. Neurosci Bull 2020;36(4):385-395.
50. El-Tanani M, Al Khatib AO, Aladwan SM, *et al.* Importance of STAT3 signalling in cancer, metastasis and therapeutic interventions. Cell Signal 2022;92:110275.
51. Tošić I, Frank DA. STAT3 as a mediator of oncogenic cellular metabolism: Pathogenic and therapeutic implications. Neoplasia 2021;23(12):1167-1178.
52. Hedl M, Sun R, Huang C, *et al.* STAT3 and STAT5 signaling thresholds determine distinct regulation for innate receptor–induced inflammatory cytokines, and STAT3/STAT5 disease variants modulate these outcomes. J Immunol 2019;203(12):3325-3338.
53. Wang YD, Miller K, Boschelli DH, *et al.* Inhibitors of Src tyrosine kinase: The preparation and structure–activity relationship of 4-anilino-3-cyanoquinolines and 4-anilinoquinazolines. Bioorg Med Chem Lett 2000;10(21):2477-2480.
54. Martellucci S, Clementi L, Sabetta S, *et al.* Src family kinases as therapeutic targets in advanced solid tumors: What we have learned so far. Cancers 2020;12(6):1448.
55. Luo J, Zou H, Guo Y, *et al.* SRC kinase-mediated signaling pathways and targeted therapies in breast cancer. Breast Cancer Res 2022;24(1):99.
56. Klyushova LS, Perepechaeva ML, Grishanova AY. The role of CYP3A in health and disease. Biomedicines 2022;10(11):2686.
57. Mitra R, Guo Z, Milani M, *et al.* CYP3A4 mediates growth of estrogen receptor-positive breast cancer cells in part by inducing nuclear translocation of phospho-Stat3 through biosynthesis of (±)-14,15-epoxyeicosatrienoic acid (EET). J Biol Chem 2011;286(20):17543-17559.
58. Xu X, Zhang XA, Wang DW. The roles of CYP450 epoxygenases and metabolites, epoxyeicosatrienoic acids, in cardiovascular and malignant diseases. Adv Drug Deliv Rev 2011;63(8):597-609.
59. Badar MS, Shamsi S, Ahmed J, *et al.* Molecular dynamics simulations: Concept, methods, and applications. In: Rezaei N, editor. Transdisciplinarity. Cham: Springer International Publishing; 2022.

60. Tallei TE, Tumilaar SG, Niode NJ, *et al.* Potential of plant bioactive compounds as SARS-CoV-2 main protease (Mpro) and spike (S) glycoprotein inhibitors: A molecular docking study. Scientifica 2020;2020:6307457.
61. Rébé C, Ghiringhelli F. STAT3, a master regulator of anti-tumor immune response. Cancers 2019;11(9):1280.
62. Maharjan CK, Mo J, Wang L, *et al.* Natural and synthetic estrogens in chronic inflammation and breast cancer. Cancers 2022;14(1):206.